Materials Transactions, Vol. 47, No. 10 (2006) pp. 2606 to 2609

RAPID PUBLICATION

Ductile Metallic Glasses in Supercooled Martensitic Alloys

J. Das[1,2,*], K. B. Kim[3], W. Xu[1], B. C. Wei[4], Z. F. Zhang[5], W. H. Wang[6], S. Yi[7] and J. Eckert[1,2]

[1]*FG Physikalische Metallkunde, FB 11 Material- und Geowissenschaften, Technische Universität Darmstadt, Petersenstraße 23, D-64287 Darmstadt, Germany*
[2]*Leibniz-Institut für Festkörper- und Werkstoffforschung Dresden, Postfach 270016, D-01171 Dresden, Germany*
[3]*Department of Advanced Materials Engineering, Sejong University, 98 Gunja-dong, Gwangjin-gu, Seoul 143-747, Korea*
[4]*Institute of Mechanics, Chinese Academy of Sciences, Beijing 100080, China*
[5]*Shenyang National Laboratory for Materials Science, Institute of Metal Research, Chinese Academy of Sciences, 72 Wenhua Road, Shenyang, 110016, P.R. China*
[6]*Institute of Physics, Chinese Academy of Sciences, Beijing 100080, China*
[7]*Department of Materials Science and Metallurgy, Kyungpook National University, Daegu 702-701, Korea*

We report ductile bulk metallic glasses based on martensitic alloys. The slowly cooled specimens contain a mixture of parent 'austenite' and martensite phase. The slightly faster cooled bulk metallic glasses with 2–5 nm sized 'austenite'-like crystalline cluster reveal high strength and large ductility (16%). Shear bands propagate in a slither mode in this spatially inhomogeneous glassy structure and undergo considerable 'thickening' from 5–25 nm. A 'stress induced displacive transformation' is proposed to be responsible for both plasticity and work-hardening-like behavior of these 'M-Glasses'. [doi:10.2320/matertrans.47.2606]

(Received June 7, 2006; Accepted August 31, 2006; Published October 15, 2006)

Keywords: *Bulk metallic glass, solidification, mechanical properties, deformation, phase transformation*

1. Introduction

Recent development of bulk metallic glasses (BMGs) has attracted enormous interest because of their potential as structural materials.[1,2] The plastic deformation process of metallic glasses is related to 'shear transformation zones' (STZs) consisting of 200–300 atoms which undergo cooperative shear.[3,4] The shear localization is a result of a rapid dilation accompanying high-rate shear deformation of short-range ordered clusters.[4,5] Localized shear transformations along certain preferred directions (*i.e.*, direction of maximum shear stress) create microstructural shear bands,[4,5] exhibiting strain softening/thermal softening.[6,7] However, failure occurs catastrophically along a single shear band without macroscopic plasticity.[8] In order to overcome the limited plastic deformability of BMGs, composite microstructures containing micrometer-size crystalline particles embedded in a glassy matrix, have been shown to be effective in order to control the plastic instability.[9–11] Recently, a large number of metallic glasses have been reported to show ductility at room tempearture.[12–15] There are a few approaches that have been proposed in order to successfully prepare ductile BMGs, like to achieve a critical value of Poisson's ratio,[13,16] or to introduce atomic-scale inhomogenities[12,14] or a phase separated glassy structure.[15,17]

In this work, we present bulk metallic glasses exhibiting large plastic deformability in supercooled Cu-Zr- and Ti-(Cu,Ni)-base martensite alloys. Our experimental evidence together with supporting literature data clearly indicates that a unique 'austenite-like' clustered glassy structure can be achieved in these alloys, which does not depend on a specific pin-pointed composition but seems to exist for a wide variety of ductile BMGs or 'M-Glasses'. A 'stress induced displacive transformation' occurs around the STZs, which releases the local stress concentration, and delocalizes the shear by forming wavy shear bands.

*Corresponding author, E-mail: j.das@ifw-dresden.de

2. Experimental

The alloys used in this work were designed from $Cu_{50}Zr_{50}$ and $Ti_{50}(Cu,Ni)_{50}$ alloys. The alloys have been prepared by mixing the pure elements in an arc melter. The ingots have been remelted several times in order to obtain homogeneity of the alloy. Rods of 2–2.5 mmϕ have been produced by solidifying *in situ* in a suction casting facility attached to the arc melter. A Zeiss DSM 962 scanning electron microscope and Philips XL 30 a high resolution SEM operated at 25 kV with an attached energy dispersive spectroscopy analysis were used for microstructure observation. A Philips CM20 transmission electron microscope (TEM) coupled with energy-dispersive X-ray analysis (EDX), differential scanning calorimetry (Perkin-Elmer Diamond DSC), and a Siemens D500 X-ray diffractometer (XRD) with Cu-K_α radiation were used for structural characterization. The TEM specimens were prepared by the conventional method of slicing and grinding, followed by ion-milling with liquid nitrogen cooling. In order to evaluate the mechanical properties under compression, cylindrical specimens with a 2 : 1 aspect ratio were prepared and tested in a Schenck servo-hydraulic testing machine under quasistatic loading at an initial strain rate of $8 \times 10^{-4}\,s^{-1}$ at room temperature. Fractographic investigation has been performed by using SEM.

3. Results and Discussion

Figures 1(a)–(e) shows the microstructure and the XRD patterns of differently solidified $Cu_{50}Zr_{50}$, $Cu_{47.5}Zr_{47.5}Al_5$

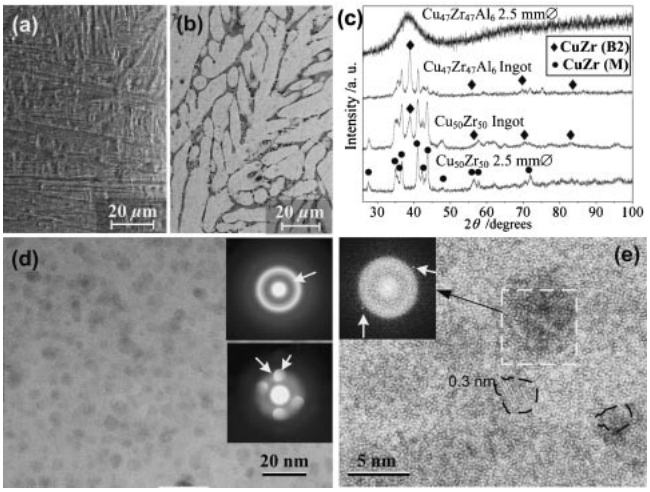

Fig. 1 SEM images of (a) $Cu_{50}Zr_{50}$, 2.5 mmϕ rod showing martensitic laths, (b) $Cu_{47}Zr_{47}Al_6$ ingot showing primary dendritic CuZr (B2) phase. (c) XRD patterns for differently solidified alloys. (d) TEM bright field image of a $Cu_{47.5}Zr_{47.5}Al_5$ glass showing a contrast, top inset: SAED pattern, bottom inset: nanobeam diffraction pattern from few darker regions shows presence of the crystallinity. (e) HREM image and FFT of the same microstructure.

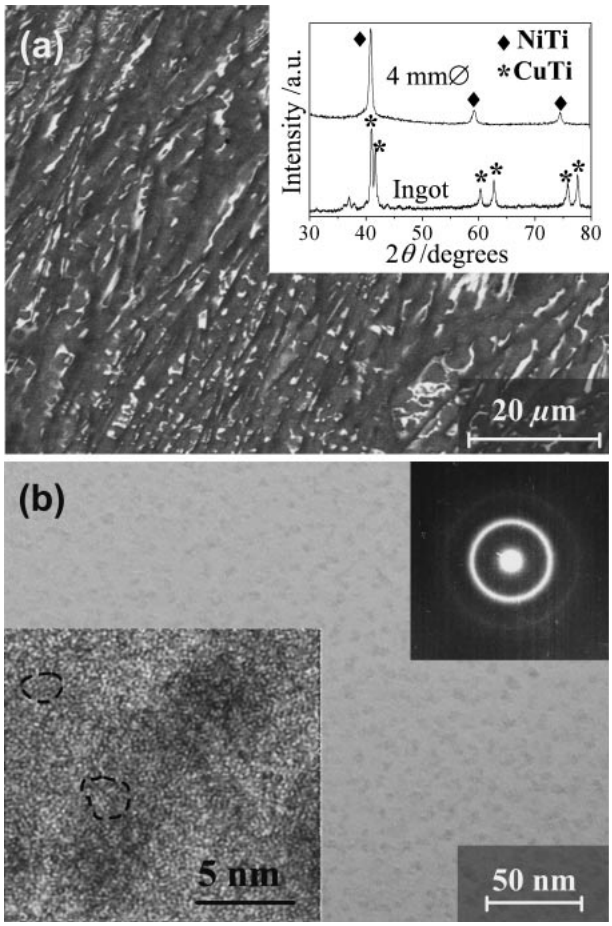

Fig. 2 (a) SEM back scattered electron image of an $Ti_{45}Cu_{40}Ni_{7.5}Zr_5Sn_{2.5}$ ingot; inset: XRD patterns of the ingot and 4 mmϕ rod; (b) TEM image of a 2 mmϕ rod revealing a clustered glassy structure (top inset, SAED pattern) and (bottom inset) HREM image indicating the presence of crystalline clusters.

and $Cu_{47}Zr_{47}Al_6$ alloys. The 2.5 mmϕ rod of $Cu_{50}Zr_{50}$ exhibit needle-shape martensite (Fig. 1(a)). The XRD pattern (Fig. 1(c)) reveals the presence of a monoclinic CuZr ($P2_1/m$ and Cm space group) martensite phase.[18] However, the slower cooled arc-melted ingot (AMI) shows a mixture of parent CuZr (B2 phase, Pm3m)[18–20] and monoclinic martensite (Fig. 1(d)). Addition of 5–6 at% Al to $Cu_{50}Zr_{50}$ shifts the composition from the line compound (CuZr) and the Cu-Zr-Al alloys solidify to a primary CuZr (B2) phase (Fig. 1(d))[20,21] and a eutectic matrix. A typical microstructure of $Cu_{47}Zr_{47}Al_6$ AMI is presented in Fig. 1(c). EDX analysis gives the average composition, the composition of dendrites and that of the eutectic matrix as $Cu_{47.3}Zr_{46.2}Al_{6.5}$, $Cu_{47.2}Zr_{46.7}Al_{6.1}$ and $Cu_{44.4}Zr_{44.7}Al_{10.9}$, respectively. $Cu_{47.5}Zr_{47.5}Al_5$ (2 mmϕ) and $Cu_{47}Zr_{47}Al_6$ (2.5 mmϕ) alloys solidified at a higher cooling rate (500-200 K/s)[22] exhibit a glassy structure, as proved by XRD (Fig. 1(d)), DSC and TEM. The glass transition temperature (T_g) of this alloy is measured to be 701 K at a heating rate of 20 K/min. It has already been reported that 5 mmϕ glassy rods can be prepared by adding 4–6 at% Al to $Cu_{50}Zr_{50}$.[23] TEM investigations reveal a contrast in the bright field images pointing to the presence of structural inhomogeneities [Fig. 1(d)]. Although the selected area diffraction pattern (SAED) (top inset, Fig. 1(d)) from such a microstructure is identified to be glassy, nanobeam (7 nm) diffraction reveals that some of the regions show twin diffraction patterns (marked by two arrows in the bottom inset, Fig. 1(d)). The Fourier filtered image [Fig. 1] shows the presence of 2–5 nm scale lattice periodicity without any sharp crystal-amorphous boundaries (marked by dashed circles, Fig. 1(e)). However, the Fast Fourier Transformation (FFT) from those darker regions (marked by a square, Fig. 1(e)) reveals the glassy nature at high resolution. In addition, the appearance of two spots in FFT (marked by arrows) indicates the presence of atomic scale order. The atomic layer spacing measured from the high resolution images is 0.3 nm, which is on the order of the (100) spacing of the CuZr B2 parent phase.

Similar features were also found for other alloys, *e.g.* for Ti-(Cu,Ni)-base glass-forming systems. The microstructure of $Ti_{45}Cu_{40}Ni_{7.5}Zr_5Sn_{2.5}$ AMI shows elongated dark and gray grains together with lamellar dark and brighter phases with an eutectic-like morphology (Fig. 2(a)). EDX analysis reveals that the average composition of the alloy is $Ti_{45.2}Cu_{40.4}Ni_{7.4}Zr_{4.6}Sn_{2.4}$. The composition of the white phase is $Ti_{34.8}Cu_{21.1}Ni_{5.4}Zr_{20.6}Sn_{18.1}$, and that of the dark and gray grains is $Ti_{47.5}Cu_{45.7}Ni_{4.8}Zr_{1.3}Sn_{0.7}$ and $Ti_{45.0}Cu_{37.3}Ni_{13.5}Zr_{3.3}Sn_{0.9}$, respectively. The XRD pattern (inset in Fig. 2(a)) from this microstructure reveals a tetragonal CuTi phase (P4-nmm) together with weak unidentified peaks. The 4 mmϕ rod of this alloy exhibits a NiTi (B2) parent phase (inset in Fig. 2(a)). This indicates that a higher cooling rate promotes the formation of the B2 phase upon solidification, as observed earlier.[24] However, the as-solidified microstructure of the 2 mmϕ rod is glassy, as proved by XRD, TEM and DSC. The glass transition temperature is 690 K (heating rate of 20 K/min). The bright field image of such a glassy structure is presented in Fig. 2(b) and the corresponding SAED pattern is shown in the inset. Despite the fact that the SAED pattern indicates a glassy structure, a contrast is

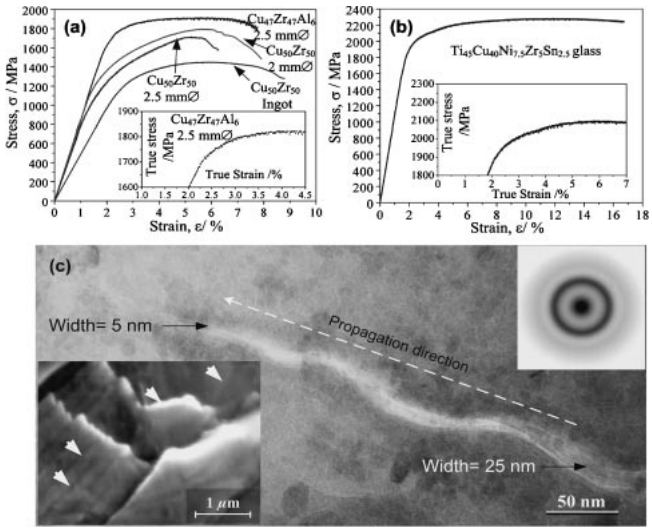

Fig. 3 Engineering stress strain curves for (a) CuZr-(Al) ductile alloys; inset: true stress-true strain curve, (b) Stress-strain curve for $Ti_{45}Cu_{40}Ni_{7.5}Zr_5Sn_{2.5}$ glass; inset: true stress-true strain curve revealing work hardening-like behavior and (c) TEM image of a deformed $Cu_{47.5}Zr_{47.5}Al_5$ glass revealing slither shear bands (right inset, the SAED pattern showing glassy phase after deformation, left inset: narrow 100–200 nm spacing appearing on the specimen surface of Ti-base glassy alloy).

observed in the bright field images. The high resolution image points to 2–5 nm size lattice periodicities similar as found for the investigated Cu-Zr-Al alloys.

The stress-strain curves of differently prepared crystalline and glassy Cu-Zr-Al alloys (Fig. 3(a)) show plastic deformation and strain hardening. The $Cu_{47.5}Zr_{47.5}Al_5$ and $Cu_{47}Zr_{47}Al_6$ glassy rods have a significantly higher yield strength ($\sigma_y = 1547$ MPa and 1687 MPa) compared to the crystalline $Cu_{50}Zr_{50}$ ingot ($\sigma_y = 1193$ MPa) and 2.5 mmϕ rods (1116 MPa) together with large plastic strain ($\varepsilon_p = 16\%$[14] and 5.5%). Interestingly, the investigated $Cu_{50}Zr_{50}$ 2 mmϕ glassy composite (Fig. 3(a)) with 10 nm sized CuZr B2 phase also displays high strength ($\sigma_y = 1272$ MPa) and work hardening up to 1794 MPa and 6.2% plastic strain. In an extreme case, more than 50% plastic strain was observed for $Cu_{50}Zr_{50}$.[25] In addition, $Cu_{46.5}Zr_{48.5}Al_5$ BMG composite specimens[20] with micrometer-size CuZr B2 phase also display strain hardening and plastic deformability. Similarly, the $Ti_{45}Cu_{40}Ni_{7.5}Zr_5Sn_{2.5}$ glass also shows high strength and large ductility ($\varepsilon_p = 16\%$) together with strain hardening behavior (inset, Fig. 3(b)).

Investigations on the microstructural evolution of shear bands indicate that the propagation pathway of these deformation bands has a definite wavy feature (Fig. 3(c)) and narrow (50–200 nm) inter-shear band spacing (left inset, Fig. 3(c)) representing a homogeneous strain distribution. It can be clearly seen from Fig. 3(c) that the wavyness of the shear band in $Cu_{47.5}Zr_{47.5}Al_5$ glass decreases along the propagation direction from right to left. The SAED pattern from this deformed region shows an amorphous halo as depicted in the right inset of Fig. 3(c) indicating that there is no nanocrystallizaion upon deformation. The shear band thickness close to the apex is about 3–5 nm, which is on the order of the size of STZs.[4] Apart from this region the thickness of the shear band is about 25 nm demonstrating a considerable 'thickening' during their propagation.

Table 1 Recently reported ductile BMGs based on martensite CuZr- and Ti(Cu,Ni)-alloy compositions.

Alloy composition /Casting thickness	Microstructure	Plastic strain (ε_p)	Reference
$Cu_{50}Zr_{43}Al_7$ (3 mmϕ)	Glassy	4.0%	15)
$Cu_{47.5}Zr_{47.5}Al_5$ (2 mmϕ)	Medium range order	16.0%	14)
$Cu_{45}Zr_{55}$ (1.5 mmϕ)	Glassy	1.5%	30)
$Cu_{55}Hf_{45}$ (1.5 mmϕ)	Glassy	2.2%	30)
$Cu_{46}Zr_{54}$ (2 mmϕ)	Glassy	1.0%	28)
$Cu_{50}Zr_{50}$ (1.5 mmϕ)	Medium range order	11.7%	27)
$Cu_{46.5}Zr_{48.5}Al_5$ (3 mmϕ)	Glassy + CuZr B2 phase	7.7%	20)
$Cu_{50}Zr_{47.5}Ti_{2.5}$ (1.5 mmϕ)	Glassy + CuZr B2 phase	8.5%	31)
$Ti_{45}Cu_{45}Ni_5Zr_5$ (3 mmϕ)	Glassy	1.8%	29)

The common microstructural features in differently solidified Cu-Zr-(Al) and Ti-(Cu,Ni) alloys clearly suggest the evolution of a parent B2 phase (austenite) at a lower cooling rate (100–10 K/s) and of a glassy phase with 2–5 nm size 'austenite-like' crystalline clusters at higher cooling rate (10^3–10^2 K/s). A stress-induced 'diffusion less shear transformation' from parent austenite to martensite in CuZr[18,19] and Ti(Ni,Cu)[26] B2 phases has already been reported. All these alloys either with micrometer-size,[20] 10 nm size B2 phase,[14] 5 nm size clustered glassy microstructure (present investigation), or medium-range ordered structure[27] exhibit strain hardening and ductility. We have surveyed a large number of ductile BMGs having alloy compositions near to the martensite alloy compositions (Table 1). Since very fine scale (5–10 nm) nanocrystal are not capable for dislocation multiplication and we did not observe any nanocrystallization in the shear bands in order to interpret strain hardening, this strongly suggests that the large ductility and the observed work-hardening is associated with some phase transformation in the spatially inhomogeneous clustered glassy microstructure, which is not considered in the STZ theory.[32]

In case of structurally inhomoheneous metallic glass based on martensitic alloys, the deformation mechanism of these STZs seems to play a crucial role for developing microstructural shear bands. A 'stress induced displacive transformation' occurs in the 'austenite-like' crystalline clusters, which releases the stress concentration around STZs and restricts free volume accumulation.[5] Spreading of such events in the undeformed regions close to the shear bands allows them to grow and leads to 'thickening'[33] from 5 nm to 25 nm. The rapid propagation of the shear bands in a spatially inhomogeneous glassy structure is hindered due to the 'phase transition', which leads to locally different shear rates[34] in the shear bands and they propagate in a slither mode. This requires a further stress to move the slither shear bands, which lead to work-hardening. The solidification of the present alloys can be understood with the help of a schematic time-temperature-transformation (TTT) diagram (Fig. 4). Slower cooling promotes the formation of the B2 parent phase which undergoes a martensitic transformation at M_s temperature. In contrast, addition of different constituents (like Al, Zr, Sn, Ni) in these rather poor glass-forming alloys

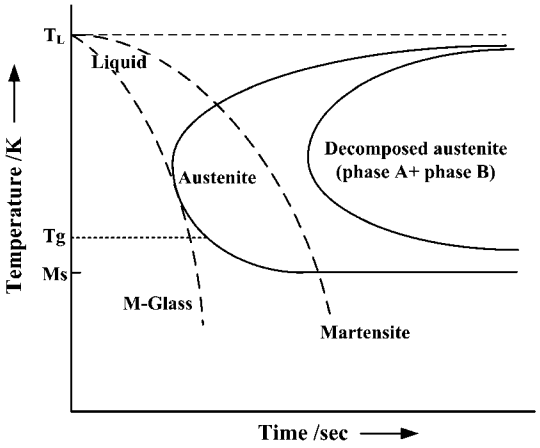

Fig. 4 Schematic time-temperature-transformation diagram of martensitic alloys illustrating the formation of ductile "work-hardenable" BMGs ('M-Glasses').

allows to vitrify the melt into an inhomogeneous glassy structure at a higher cooling rate (10^3-10^2 K/s) with stress induced martensitic transformation characteristics ('M-Glass').

4. Conclusions

A novel group of Cu-Zr- and Ti(Cu,Ni)-base ductile work-hardenable BMGs based on 'supercooled martensitic alloys' has been reported. The unique structure of the BMGs consists of ordered 'austenite-like' crystalline clusters, which are believed to induce a 'stress induced displacive transformation' at the neighbouring zone of STZs to release the local stress concentration and delocalize the shear. The shear bands thicken in a spatially inhomogeneous glassy microstructure and appear as 'wavy features' on a nanometer length scale. We believe that highly deformable metallic glasses with such a spatially inhomogeneous glassy structure can be obtained in Ni-Zr, Ni-Ti, Fe-Ni, Fe-Pt, Ti-Pt and several other near-martensitic alloys.

Acknowledgements

The authors thank A. Gebert, A. L. Greer, W. L. Johnson, U. Kunz, H. Lehmann, S. Scudino, R. Theissmann, S. Venkataraman, A. R. Yavari, P. Yu, L. C. Zhang and W. Y. Zhang for technical assistance and stimulating discussions. Funding by the EU-RTN on "ductile BMG composites" (MRTN-CT-2003-504692) is gratefully acknowledged. This work was also supported by the Korean Ministry of Commerce, Industry and Energy and Natural Science Foundation of China (Grant No. 50321101).

REFERENCES

1) A. Inoue: Acta Mater. **48** (2000) 279–306.
2) W. L. Johnson: Mater. Sci. Forum **225** (1996) 35–49.
3) W. L. Johnson and K. Samwer: Phys. Rev. Lett. **95** (2005)195501 1–4.
4) J. S. Langer: Phys. Rev. E **64** (2001) 011504 1–4.
5) F. Spaepen: Acta Metall. **25** (1977) 407–415.
6) J. J. Lewandowski and A. L. Greer: Nature Mater. **5** (2006) 15–18.
7) H. Chen, Y. He, G. J. Shiflet and S. J. Poon: Nature **367** (1994) 541–543.
8) H. A. Bruck, T. Christman, A. J. Rosakis and W. L. Johnson: Scripta Metall. Mater. **30** (1994) 429–434.
9) C. C. Hays, C. P. Kim and W. L. Johnson: Phys. Rev. Lett. **84** (2000) 2901–2904.
10) U. Kühn, J. Eckert, N. Mattern and L. Schultz: Appl. Phys. Lett. **80** (2002) 2478–2480.
11) G. He, J. Eckert, W. Löser and L. Schultz: Nature Mater. **2** (2003) 33–37.
12) L. Q. Xing, Y. Li, K. T. Ramesh, J. Li and T. C. Hufnagel: Phys. Rev. B **64** (2001) 180201.
13) J. Schroers and W. L. Johnson: Phys. Rev. Lett. **93** (2004) 255506 1–4.
14) J. Das, M. B. Tang, K. B. Kim, R. Theissmann, F. Baier, W. H. Wang and J. Eckert: Phys. Rev. Lett. **94** (2005) 205501 1–4.
15) D. S. Sung, O. J. Kwon, E. Fleury, K. B. Kim, J. C. Lee, D. H. Kim and Y. C. Kim: Metals Mater. Int. **10** (2004) 575–579.
16) J. J. Lewandowski, W. H. Wang and A. L. Greer: Phil. Mag. Lett. **85** (2005) 77–87.
17) J. C. Oh, T. Ohkubo, Y. C. Kim, E. Fleury and K. Hono: Scripta Mater. **53** (2005) 165–169.
18) D. Schryvers, G. S. Firstov, J. W. Seo, J. VanHumbeeck and Y. N. Koval: Scripta Mater. **36** (1997) 1119–1125.
19) Y. N. Koval, G. S. Firstov and A. V. Kotko: Scripta Metall. Mater. **27** (1992) 1611–1616.
20) Y. F. Sun, B. C. Wei, Y. R. Wang, W. H. Li, T. L. Cheung and C. H. Shek: Appl. Phys. Lett. **87** (2005) 051905 1–3.
21) D. Wang, H. Tan and Y. Li: Acta Mater. **53** (2005) 2969–2979.
22) R. M. Srivastava, J. Eckert, W. Löser, B. K. Dhindaw and L. Schultz: Mater. Trans., JIM **43** (2002) 1670–1675.
23) P. Yu, H. Y. Bai, M. B. Tang and W. L. Wang: J. Non-Cryst. Solids **351** (2005) 1328–1332.
24) T. G. Woodcock, M. Kusy, S. Mato, G. Alcala, J. Thomas, W. Löser, A. Gebert, J. Eckert and L. Schultz: Acta Mater. **53** (2005) 5141–5149.
25) A. Inoue, W. Zhang, T. Tsurui, A. R. Yavari and A. L. Greer: Phil. Mag. Lett. **85** (2005) 221–229.
26) D. Schryvers and R. Santamarta: Scripta. Mater. **50** (2004) 1423–1427.
27) Z. W. Zhu, H. F. Zhang, W. S. Sun, B. Z. Ding and Z. Q. Hu: Scripta Mater. **54** (2006) 1145–1149.
28) D. C. Hofmann, G. Duan and W. L. Johnson: Scripta Mater. **54** (2006) 1117–1122.
29) H. Men, S. J. Pang, A. Inoue and T. Zhang: Mater. Trans., JIM **46** (2005) 2218–2220.
30) A. Inoue and W. Zhang: Mater. Trans., JIM **45** (2004) 584–587.
31) Q. Zhang, H. Zhang, Z. Zhu and Z. Hu: Mater. Trans., JIM **46** (2005) 730-73.
32) M. L. Falk and J. S. Langer: Phys. Rev. E **57** (1998) 7192–7205.
33) K. Hajlaoui, A. R. Yavari, B. Doisneau, A. LeMoulec, W. J. Botta F., G. Vaughan, A. L. Greer, A. Inoue, W. Zhang and Å. Kvick: Scripta Mater. **54** (2006) 1829–1834.
34) J. B. Salmon, S. Manneville and A. Colin: Phys. Rev. E **68** (2003) 051503 1–12.